JOURNAL OF GUIDANCE, CONTROL, AND DYNAMICS
Vol. 30, No. 2, March–April 2007

Enhanced Self-Spacing Algorithm for Three-Degree Decelerating Approaches

J. L. De Prins,* K. F. M. Schippers,† M. Mulder,‡ M. M. van Paassen,§ and A. C. in't Veld‖
Delft University of Technology, 2629 HS Delft, The Netherlands
and
J.-P. Clarke¶
Georgia Institute, of Technology, Atlanta, Georgia 30332

DOI: 10.2514/1.24542

A current trend in aircraft noise abatement around airports is exploiting the benefits of revised arrival and approach procedures with computational aids, such as onboard and ground-based trajectory prediction algorithms and displays. The challenge for these upcoming advanced noise abatement procedures is to mitigate the noise impact without sacrificing runway capacity. A proposed solution, implemented in the three-degree decelerating approach, is to delegate the task of spacing the aircraft to the cockpit during the approach. To assist the pilots, a flap scheduling algorithm with complementary interface has been developed that takes noise nuisance and in-trail spacing into account. The design and functionality of this support system is presented and evaluated with three experiments. Monte Carlo simulations indicated adequate and consistent performance and robustness of the self-spacing algorithm for various wind and traffic scenarios. A pilot-in-the-loop simulator experiment verified that, with the aid of the algorithm, pilots were able to execute the noise abatement procedure consistently while maintaining safe spacing. The support system reduced pilot workload up to an effort level comparable to current standard approaches. The concept was demonstrated in flight, which confirmed the conflict-free performance benefits and the feasibility of self-spacing during continuous decelerating/descent approaches under actual flight conditions.

Nomenclature

h_{APP}	=	target approach altitude, ft
h_{TCB}	=	thrust-cutback altitude, ft
$h@V_{APP}$	=	altitude at which V_{APP} is reached, ft
V_{APP}	=	final approach speed (indicated airspeed), kn
$\Delta spacing_{safe}$	=	minimum actual spacing with respect to required safe separation, NM

I. Introduction

SEVERAL advanced noise abatement procedures (ANAPs) have been developed, evaluated, and continuously improved over the last few years. These include the continuous descent approach (CDA) [1–8] the prototypes of which are already operational at a few airports during nighttime (for example, at Amsterdam Schiphol Airport, London Heathrow, Frankfurt, Stockholm Arlanda), the low power/low drag approach (LP/LD) [8–10], the two-segment approach (TSA) [10–12], the advanced continuous descent approach [13,14] and the three-degree decelerating approach (TDDA) [15]. The noise impact and operational characteristics of these procedures have been validated through several piloted simulator experiments [4,10,12] and the recent flight demonstration tests of the CDA procedure at Louisville International Airport [5,16]. Although successful in reducing noise, runway capacity problems have restricted the implementation of the noise abatement procedures to the lower traffic density hours [1,8]. The main reason is the inability of air traffic control (ATC) to properly space aircraft that are decelerating at significantly different rates [17]. To compensate for these uncertainties, controllers apply larger spacing than normal resulting in a capacity loss with respect to conventional approaches [18].

A possible solution to decrease the distances between arriving aircraft is to delegate the spacing task to the pilot. Although the air traffic control retains overall responsibility of aircraft separation, they would only monitor the decelerating traffic and intervene when aircraft do not conform to their respective trajectories [18]. In in't Veld et al., an onboard automated tool took into account minimum spacing constraints with the preceding aircraft when determining the flap position changes during a three-degree decelerating approach procedure. A pilot support interface was developed to present the output of the flap scheduling algorithm. Piloted simulator experiments indicated that the algorithm performs adequately in zero-wind conditions and is beneficial, especially in off-nominal traffic scenarios [18] (i.e., when the aircraft in front deviates from its nominal speed profile by decelerating earlier). These promising research results motivated the enhancement of the flap scheduling algorithm to expand its general performance and applicability in multiple wind conditions [19], and the evaluation of the feasibility of self-spacing during decelerating approaches under actual flight conditions. Although this research work focuses on distance-based spacing, a parallel line of research adapted and evaluated the enhanced flap scheduling algorithm for time-based spacing applications, and augmented the prediction algorithm with an advanced statistical based wind profile estimator [20].

The purpose of this paper is twofold. First and foremost, this paper will describe in-depth the design and functionality of the enhanced

Presented as Papers 6139 and 6140 at the AIAA Guidance, Navigation, and Control Conference and Exhibit, San Francisco California, 15–18 August 2005; received 10 April 2006; accepted for publication 4 August 2006. Copyright © 2006 by Delft University of Technology. Published by the American Institute of Aeronautics and Astronautics, Inc., with permission. Copies of this paper may be made for personal or internal use, on condition that the copier pay the $10.00 per-copy fee to the Copyright Clearance Center, Inc., 222 Rosewood Drive, Danvers, MA 01923; include the code 0731-5090/07 $10.00 in correspondence with the CCC.

*Research Associate, Control and Simulation Division/Aerospace Software and Technologies Institute, Faculty of Aerospace Engineering, Kluyverweg 1; j.l.deprins@tudelft.nl.

†Research Associate, Control and Simulation Division, Faculty of Aerospace Engineering, Kluyverweg 1; kristof.schippers@eurocontrol.int

‡Associate Professor, Control and Simulation Division, Faculty of Aerospace Engineering, Kluyverweg 1; m.mulder@tudelft.nl. Member AIAA.

§Associate Professor, Control and Simulation Division, Faculty of Aerospace Engineering, Kluyverweg 1; m.m.vanpaassen@tudelft.nl. Member AIAA.

‖Research Associate, Control and Simulation Division, Faculty of Aerospace Engineering, Kluyverweg 1; a.c.intveld@tudelft.nl.

¶Associate Professor, School of Aerospace Engineering, Georgia Institute of Technology, Atlanta, Georgia; john-paul.clarke@ae.gatech.edu. Member AIAA.

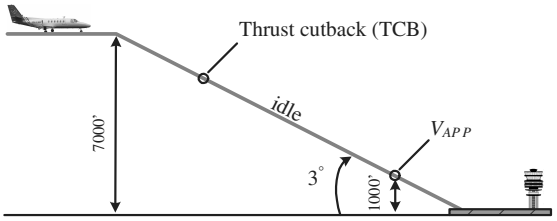

Fig. 1 The three-degree decelerating approach.

flap scheduling algorithm. Second, this paper will present the results of three experiments that were conducted to validate the algorithm: a Monte Carlo simulation experiment evaluating the algorithm performance in various wind and traffic scenarios and its sensitivity to relevant prediction errors [19]; proof of concept flight test experiment demonstrating the viability of the algorithm in real flight [21]; pilot-in-the-loop simulator experiment investigating operational performance and benefits of the support system, including workload assessment, when pilots are involved in a self-spacing task during a TDDA [21].

II. Three-Degree Decelerating Approach and Support System

A. Approach Procedure

In a TDDA, illustrated in Fig. 1, aircraft descend along a fixed 3 deg flight path to the runway, starting at higher altitude and at higher speeds than the conventional ILS approach (where aircraft descend along a 3 deg flight path after a level flight at 2000–3000 ft). For example, initial altitude and speed could be 7000 ft and 250 kn, respectively. Top-of-descent and aircraft cruising speed are possible as well. Speed reductions are achieved by applying idle thrust during the descent and letting the aircraft decelerate along the fixed glide path according to the existing drag forces. This aerodynamic drag is controlled with the selection of flaps and gear. Ultimately, the aircraft should reach the final approach speed V_{APP} [in indicated airspeed (IAS)] and be into a complete stabilized landing configuration at the reference height h_{APP} of 1000 ft above the runway, without the application of thrust [18]. At this point, thrust can be added to land the aircraft following common procedure. To aid the pilot with managing the aircraft configuration and longitudinal spacing, a flap scheduling algorithm has been designed.

B. Optimization Algorithm

The moment at which engine thrust must be reduced and the next flap setting or gear must be extended is accurately calculated by a flap optimization algorithm. The flap scheduling routine has two objectives. First, minimum safe spacing with the preceding aircraft must be assured, that is, 2.5 NM in the case of two light aircraft trailing each other [17]. Second, the flap/gear schedule should be optimized such that the target speed V_{APP} is reached at the reference altitude h_{APP} without additional thrust. These two objectives will be referred to as, respectively, the *spacing goal* and the *noise goal*.

Although reaching V_{APP} below h_{APP} is more beneficial for noise production, the noise goal has been augmented with the constraint that aircraft should be fully established in landing configuration as close to h_{APP} as possible. Therefore, reengaging thrust below h_{APP} will be associated with decline in "noise" performance.

Because the TDDA is executed with idle thrust along a fixed flight path, the timing of thrust cutback, flap and gear selection are the only control options to properly achieve the goals. Speed brakes are envisioned as a backup control alternative. The use of speed brakes is undesired because it increases airframe noise significantly. During the descent, the number of control options gradually decreases as thrust is fixed at idle and flaps are selected one by one. Consequently, it is desirable to keep the largest control authority for the latest flap setting, in both tuning directions, such that the algorithm is still able to correct unexpected deviations during the final part of the TDDA. Hereby, the performance of the TDDA objectives can be maximized. The complete flap-tuning algorithm is elaborated in detail in Sec. III.

C. Pilot Support Interface

To support pilots in their task of flying the TDDA, cues have been added to the primary flight display (PFD) and navigation display (ND) [18,21]; see Fig. 2. A green thrust cue "T" on the altitude indicator displays the thrust cutback altitude. A green Flap cue "F" on the airspeed indicator indicates the speed of the aircraft at which the next flap is to be selected. A yellow "G" cue exhibits the optimized speed at which the landing gear is to be extended. The calculated airspeed at which the flap or gear should be extended is shortened to the term *flap speed* and *gear speed* in the remainder of this paper. When speed brakes or thrust are required, "ADD DRAG" or "ADD THRUST" annunciations pop-up.

The navigation display is provided with continuous information about aircraft in the vicinity using standard traffic alert and collision avoidance system symbology. Additionally, the display has been augmented with continuously updated information (1 Hz) on the future spacing trend by adding a *predicted spacing arc* [21]. The spacing arc indicates the difference between predicted spacing at the threshold and minimum safe spacing with respect to the current position of the lead aircraft. Thus, when the arc is behind the lead aircraft, safe spacing is guaranteed. On the other hand, an arc encapsuling the lead indicates future violation of safe spacing. In this way, the spacing arc serves as an interactive safety corridor, which facilitates pilot's interpretation of the situation.

III. Enhanced Three-Degree Decelerating Approach Algorithm

A prediction and optimization algorithm was developed [14,18] and enhanced [19] to aid the pilot with his self-spacing task and his task of arriving at the reference height with V_{APP}. The algorithm determines at what altitude thrust should be reduced and at what speed each flap setting and the gear should be selected. A detailed description is presented in this section of the algorithm's prediction methods and control laws to satisfy the noise and spacing goals simultaneously under a range of atmospheric conditions.

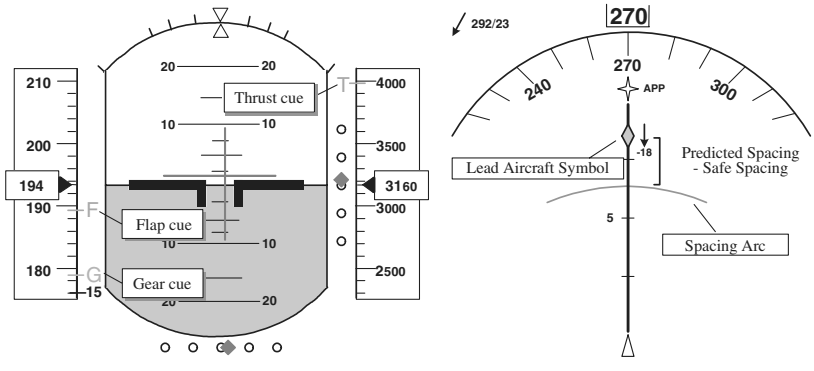

a) b)

Fig. 2 a) Primary flight display (PFD) and b) navigation display (ND), extended with cues from the pilot support system.

A. Structure of the Flap Optimization Algorithm

The design of the flap optimization algorithm is illustrated in Fig. 3. First, the trajectory of the lead aircraft is predicted. Next, a prediction of the own trajectory is made given the last calculated flap schedule, current aircraft state and estimated wind. Both traces are then compared, yielding the predicted spacing trend. If spacing is expected to be violated, the flap selection timing is tuned to slow down earlier and hence increase spacing. To determine the proper flap speeds, the iteration process first distinguishes between the situations where the aircraft is above or below the thrust cutback altitude (h_{TCB}). These situations correspond to the CAPTURE mode and the HOLD mode of the flap scheduler, respectively:

1) In CAPTURE mode, the algorithm calculates the altitude at which the thrust should be set to flight-idle (h_{TCB}). This altitude is determined using *start altitude optimization* such that safe spacing is assured while still being able to reach the reference height without applying thrust. As soon as the calculated start altitude is reached, the algorithm switches to HOLD mode.

2) In HOLD mode, the flap scheduler uses *noise and traffic (NT) optimization* to adjust the flap/gear speeds. If, however, in this part of the approach spacing is predicted to be violated, the noise and spacing goals are decoupled, that is, flaps must be extended at higher speeds to decelerate earlier and increase spacing. Consequently, the aircraft will get to V_{APP} early and extra thrust will be required. The algorithm will now primarily tune the flaps to guarantee safe spacing.

The flap schedule tuning process is a binary search algorithm [18], starting with a coarse flap-tuning routine, followed by a fine-tuning process to determine a flap schedule that satisfies the applicable constraint (spacing or noise). During coarse tuning, the first flap stage is set to its upper/lower bound, followed by the next flap and so on until the relevant constraint is overcorrected. At each adjustment, the trajectory and spacing trends are recalculated to check with the constraints. The upper and lower bounds for each flap speed are given by the flap placard speed and the minimum manoeuvring speed, respectively. Applicable constraints are further discussed in the description of the NT optimization in Sec. III.F. When the relevant criterion is exceeded, the last adjusted flap setting is fine tuned to get the constraint within its margins. Fine tuning is done by setting the last tuned flap speed to the midpoint between the nominal speed and the last set boundary. This process of setting the flap speed halfway between the current midpoint and the previous boundary is repeated until the applicable constraint is met. It is noted that the term "optimization" is not entirely correct as the automated tool does not search for the most optimal flap schedule, but rather a satisfactory one, possibly with a small sacrifice in noise abatement; therefore, "satisficing" would be a better expression [22].

In case flap tuning fails to ensure safe spacing or to reach the target speed, the timing of extending the landing gear is a final control variable that can be adjusted by the optimization algorithm. The tuning of the gear speed works identical to the flap tuning. When even the landing gear adjustments are insufficient, speed brakes or thrust must be applied and the ADD DRAG or ADD THRUST annunciations are shown on the PFD. As a safety precaution, the ADD THRUST annunciation is also shown as soon as V_{APP} is reached.

This iteration is repeated every second to compensate for changing wind conditions and deviations from the optimal speed profile. Each element of the algorithm will be treated in more detail in the following.

B. Trajectory Prediction of the Leading Aircraft

To assess the future spacing trend between the own aircraft and the predecessor, the flap scheduler needs to accurately estimate the trajectory of the leading aircraft. Its expected trace can be determined by treating the lead as a black box, that is, without knowledge of the aircraft type and its specific aerodynamic and performance characteristics, and predicting its future speed and position profile solely based on Automatic Dependent Surveillance-Broadcast (ADS-B) data [18].

1. Prediction Method

The lead state-vector information, broadcast every second via ADS-B, is received onboard and stored. The trajectory prediction algorithm then fits a fourth order polynomial through these data using a least-square error fit and extrapolates these data to get future speed and distance trends, as presented in Fig. 4. The extrapolated speed profile is cut off at the point where V_{APP} is reached. This process is executed after each ADS-B update.

The accuracy of the speed profile prediction could be increased if ADS-B will broadcast both the lead's current state-vector and intent information [18]. For a TDDA, the intent information could consist of the lead target speed $V_{\mathrm{APP},l}$ and corresponding reference altitude $h_{\mathrm{APP},l}$. The latter can be easily transformed to the reference position $x_{\mathrm{APP},l}$ given the 3 deg glide path angle. Adding this extra data point to the historical data provides a more accurate fit, as illustrated in Fig. 4.

The intent information, however, cannot be used in the time domain because the time at which the lead reaches $V_{\mathrm{APP},l}$ is unknown. To work around this problem, $V_{\mathrm{APP},l}$ (IAS) is converted to $V_{g_{\mathrm{APP},l}}$ (groundspeed). Using the groundspeed V_g as the derivative of the traveled distance (and thus position x), the resulting first order ordinary differential equation can be solved:

$$\left.\begin{aligned} V_g &= \dot{x} \\ V_g &= f(x) \end{aligned}\right\} \qquad \dot{x} = f(x) \tag{1}$$

where $f(x)$ is the polynomial fit through the known data points in the $x - V_g$ plane of Fig. 4. Next, the predicted lead trace is constructed in the time domain using the Runge–Kutta numerical integration routine with a time step of 0.1 s. The lead's current position is the starting point of the integration. The routine iterates until the lead approach speed $V_{g_{\mathrm{APP},l}}$ is reached.

The accuracy of the prediction is further improved by passing the ADS-B data through a sliding gain filter [18]. Older data are filtered

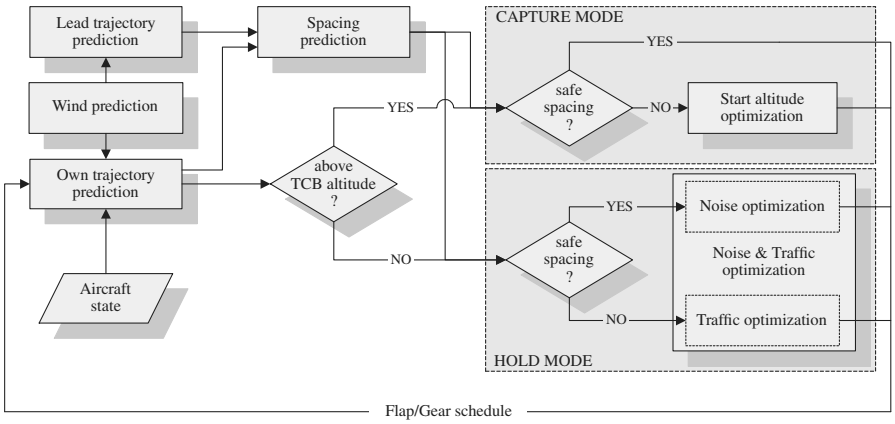

Fig. 3 Structure of the flap scheduler algorithm.

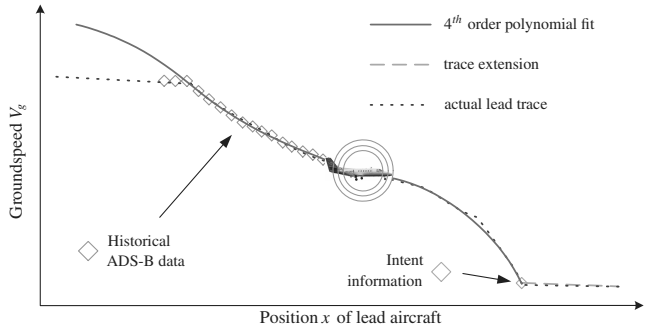

Fig. 4 Speed profile prediction of the leading aircraft.

out: only the most recent 100 data points are used. The intent information is weighed 10 times as much as a normal measurement.

The speed profile prediction described above only generates the decelerating segment of the approach until $V_{\mathrm{APP},l}$ is reached. Then the lead is expected to maintain this speed along the ILS track to the runway, as depicted in Fig. 4. Therefore, a path with constant indicated airspeed $V_{\mathrm{APP},l}$ and corresponding traveled distance is added to the predicted speed and distance profile described above.

2. Accuracy of the Prediction

The error in the lead trajectory prediction varies with the following:

1) The governing wind condition;

2) The number of data points received. If enough data are not available, the prediction deviates and is unusable. Hence, the lead trajectory is generated as soon as 80 data points are available, that is, after 80 s into the approach. In a continuous stream of arriving air traffic, the aircraft are initially spaced approximately two minutes apart. Hence, enough lead data are already available to estimate an accurate lead trajectory at the beginning of the TDDA. The accuracy increases when more data points become available.

3) The length of the time interval over which the extrapolation is carried out. The prediction accuracy increases closer to the runway because cumulative errors have less time to grow.

4) The deceleration characteristics of the lead type. This effect is elaborated further in the next section.

3. Correction to Prediction Algorithm

Although the approach for the lead's speed profile prediction proved to be accurate in simulations for a Boeing 737 lead aircraft [18], the performance of the prediction method with a fourth order polynomial decreased with a Cessna C500 Citation I lead type. The predicted spacing deviated up to a few nautical miles and decreases well below the minimum safe value of 2.5 NM. Consequently, the algorithm was unable to determine a proper thrust cutback altitude that satisfies the noise goal in addition to the spacing goal. The described diverging prediction is caused by a temporary underestimation of the lead's speed profile.

An impression of the effect in zero-wind conditions is given in Fig. 5. Because of the convex part in the deceleration profile of the Citation I model (dotted line), the algorithm temporarily creates a convex fourth order extrapolation between the historical data and intent information (dash–dotted line). This convex deceleration characteristic is not present in the 737 speed profile [18]. Although the algorithm corrects the polynomial fit for the lead aircraft known $V_{\mathrm{APP},l}$ [fine solid line 2)], it underrates the lead's ground speed to a large extent and consequently also the spacing trend, as clearly indicated in the second plot of Fig. 5.

A third order polynomial naturally consists of a convex and concave segment, and so it is not a valid solution. A second order polynomial is forced into the concave curvature due to the initial constant speed segment and therefore reduces the temporary underestimation of the fourth order prediction to a large extent, as shown in Fig. 5 [bold solid line 1)]. However, it results in a less accurate prediction of the spacing trend later during the approach.

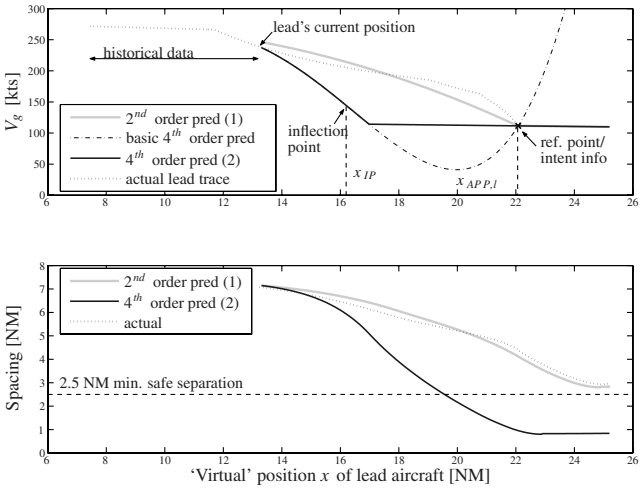

Fig. 5 Speed profile prediction of leading aircraft and resulting prediction of the spacing.

Therefore, it was decided to keep the more accurate fourth order polynomial but switch over to a second order prediction when underestimation is identified. The trigger for this correction is the position of one of the inflection points of the polynomial: a relatively good polynomial is found as long as the inflection point x_{IP} lies to the right of the reference point $x_{\mathrm{APP},l}$ ($x_{\mathrm{IP}} > x_{\mathrm{APP},l}$), or, in other words, when the second derivative of the polynomial at $x_{\mathrm{APP},l}$ is negative (concave). As soon as the second derivative gets positive (convex), the polynomial is reduced to a second order one until the inflection point moves back to the right of the reference point. This correction is sufficient to diminish the divergence in predicted spacing and makes the algorithm able to combine adequate noise and spacing performance.

C. Own Trajectory Prediction

The own trajectory is determined using a simple aerodynamic model [18] so that the speed profile can be calculated multiple times per second.

1. Aerodynamic Model

The aerodynamic model is a "point mass" aircraft model with constant mass that includes only the forces in the vertical plane (2D). The addition of wind generates a small difference between kinematic flight path angle γ_k and aerodynamic flight path angle γ_a as presented in Fig. 6. γ_k corresponds to the 3 deg ILS glide path. γ_a can be determined using two-dimensional geometry from the true airspeed V_a, defined in the aerodynamic reference frame $\mathcal{F}_a$, and the current groundspeed $\dot{x}_e$ and along-track wind speed component u_{w_e}, both defined in the local geodetic reference frame $\mathcal{F}_e$ (north-east-down), while assuming no vertical wind component:

$$\gamma_a = \arccos\left(\frac{\dot{x}_e - u_{w_e}}{V_a}\right) \tag{2}$$

where V_a can be calculated according to

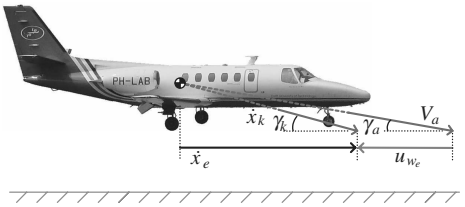

Fig. 6 The difference between kinematic flight path angle γ_k and aerodynamic flight path angle γ_a.

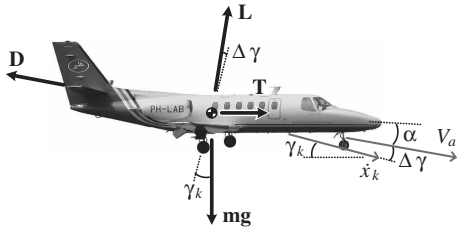

Fig. 7 Force diagram for "point mass" aircraft model.

$$V_a = \sqrt{(\dot{x}_e - u_{w_e})^2 + (\dot{x}_e \tan \gamma_k)^2} \tag{3}$$

The changing aerodynamic flight path angle causes a small component of the lift force to appear along the 3 deg glide path. Because of the low speed envelope of the Cessna C500 Citation I, $\Delta\gamma$ ($=\gamma_k - \gamma_a$) is relatively large for a Citation (0.54 deg at V_{APP} with a 20 kn headwind in comparison to, for example, 0.4 deg for a B747). This, in combination with a higher lift-over-drag ratio of the C500, implies that the resulting lift component along the flight path cannot be neglected with respect to the thrust and drag force.

Using the force diagram of Fig. 7 and given the limited angle of attack α (<5 deg) in combination with a small idle thrust compared with the other forces ($T\cos\alpha \approx T$, $T\sin\alpha$ is negligible with respect to the weight), the following equations of motion can be derived in the kinematic reference frame $\mathcal{F}_k$ [23] along the fixed flight path:

$$\begin{aligned} \Sigma F_z\colon\ & 0 = L\cos\Delta\gamma - mg\cos\gamma_k + T\sin\Delta\gamma - D\sin\Delta\gamma \\ \Sigma F_x\colon\ & m\ddot{x}_k = -L\sin\Delta\gamma + mg\sin\gamma_k + T\cos\Delta\gamma - D\cos\Delta\gamma \end{aligned} \tag{4}$$

Equations (4) hold if the aircraft is assumed to fly at a constant 3 deg approach angle (γ_k) and no turns are made. To simplify the calculation of the lift L, the vertical equilibrium of Eqs. (4) is further reduced by omitting the relatively small thrust and drag components ($T\sin\Delta\gamma$ and $D\sin\Delta\gamma$). As mentioned above, the contribution of $L\sin\Delta\gamma$ in the "horizontal" force equilibrium is essential due to the magnitude of the lifting force.

The lift L easily yields the lift coefficient C_L, which is subsequently used to calculate the drag coefficient C_D with an approximation of the drag polar:

$$C_D = c_1 C_L^2 + c_2 C_L + c_3 \tag{5}$$

where the coefficients c_1, c_2, and c_3 are dependent on flap and gear setting.

During the TDDA, the engine setting remains idle. Idle thrust primarily depends on the flap position and the true airspeed. Altitude and temperature effects are neglected. The thrust can be calculated using the following second order polynomial:

$$T = t_1 V_a^2 + t_2 V_a + t_3 \tag{6}$$

Model evaluation indicated that coefficients t_1 and t_2 are fixed per flap/gear position. The value of t_3, however, depends on the airspeed at which flaps and gear are set. Therefore an initial estimate is taken for t_3 given the nominal flap schedule. To improve the thrust estimation during the approach, the predicted idle thrust curves are constantly corrected using current calculated thrust. This *thrust-prediction-error limiter* substitutes the momentary thrust and true airspeed in Eq. (6), yielding an updated t_3 every second.

With Eqs. (2–6), the acceleration along the flight path $\ddot{x}_k$ can be determined. This acceleration is then integrated in time with a time step of 1 s, following the scheme of Fig. 8, yielding the predicted speed and distance trajectories.

2. *Calculation Direction*

The prediction model in Fig. 8 can create the trajectory in two directions by setting the proper initial constraint ($\overline{x}_{\text{start}}, \dot{\overline{x}}_{\text{start}}$). It can start at h_{APP} with V_{APP} and calculate backwards until the current airspeed is reached (*back calculation*). Or, the model can start at the current height and airspeed and predict the decelerated descent to V_{APP} (*forward calculation*). The switching between both methods is easily done in real time by just swapping the initial and end constraints, and adding a minus sign on the left-hand side of the longitudinal equation of motion in case of back calculation.

Both methods have their particular advantages. When a time-dependent wind profile estimation is used [20], the back-calculation method needs to know the time when the aircraft is at the reference height. But, to determine that time, the aircraft trajectory must be known. Hence, forward calculation, which starts at current time, is preferred. However, forward calculation is not useful to determine the thrust cutback altitude, because this would require multiple iteration loops until the right altitude is found. Therefore, the use of back calculation is preferred in CAPTURE mode, which needs only one iteration. Naturally the problem of the unknown time-at-h_{APP} remains. The proposed solution is to take an initial estimate of that time and update it every iteration loop using the calculated time at h_{APP} from the last iteration.

3. *Trace Extensions*

The aerodynamic model determines the trajectory only during the decelerating part of the descent. To get a complete trajectory prediction, the own trajectory is extended in two ways. Above the thrust cutback altitude, a constant speed segment is added from the current altitude to h_{TCB}, corresponding to the aircraft's actual indicated airspeed. Below the reference height, when thrust is reapplied, a segment of constant indicated airspeed V_{APP} is added after the trace to the runway.

D. Spacing Trend Prediction

With the predicted trajectories for the lead and own aircraft, the spacing trend can be calculated. Because the spacing trend shows "closing characteristics," the minimum predicted spacing is found at or near the runway threshold. No additional smoothing filter is required.

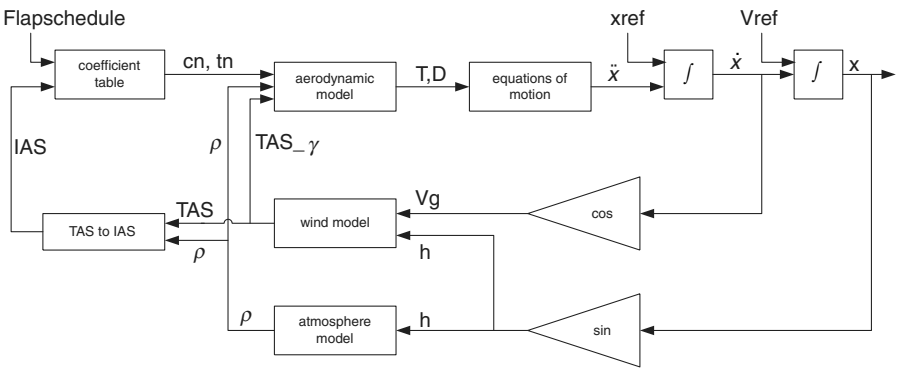

Fig. 8 Own trajectory prediction model.

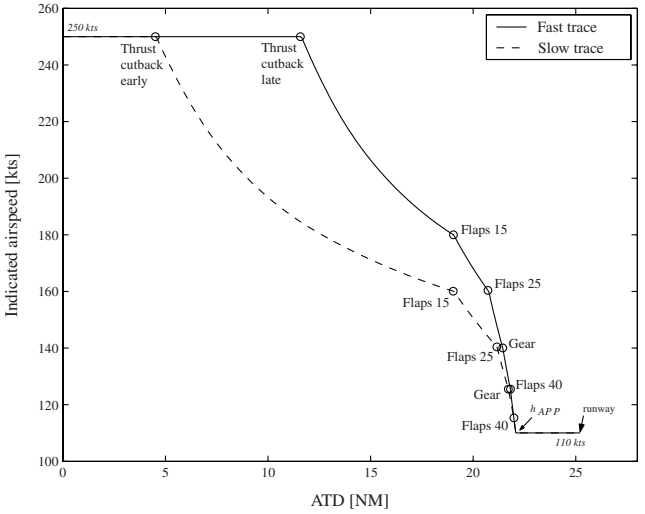

Fig. 9 Indicated airspeed as function of along-track distance (ATD) for a fast and slow approach with the Citation I in zero wind.

E. Start Altitude Optimization

Minimum noise performance is achieved in combination with safe in-trail spacing by optimizing the start altitude h_{TCB}. The idea is to alter h_{TCB} in such a way that minimum predicted spacing increases to a safe level while still being able to reach the target speed without applying thrust. The start altitude optimization process only alters h_{TCB} when spacing is predicted to get dangerous (Fig. 3). When safe spacing is guaranteed, no actions are taken. In case of excess spacing, the algorithm could also schedule a lower h_{TCB}. However, this requires further investigation into the design of the algorithm's control laws to achieve similar performance results as for the Monte Carlo simulations that were conducted (Sec. IV).

Although spacing is increased in HOLD mode by extending flaps sooner (at higher airspeeds), the approach for the start altitude optimization is completely opposite. To increase spacing, the time to fly the approach must be longer, which corresponds to a lower mean airspeed of the own aircraft throughout the approach. This can only be achieved by decelerating earlier, or in other words, increasing the thrust cutback altitude. Because the same amount of kinetic energy must be dissipated and deceleration has been started earlier, the parts of the approach with high deceleration rates (i.e., the segments at the end of the approach, flown with higher flap positions) must be shortened. Consequently, the flap speeds must be *lowered*. Figure 9 illustrates the difference between a "fast" and a "slow" approach.

The start altitude optimization tunes the flap speeds every second in such a manner that the minimum predicted spacing shifts within a distance margin of 0.05 to 0.1 NM above minimum safe spacing. This range is chosen to keep a safety margin with respect to the minimum safe spacing on the one hand (to cover inaccuracies of the lead aircraft trajectory prediction), and to avoid too large, unnecessary deviations from the nominal TDDA descent profile on the other hand. For the latter, it is best to avoid too low flap speeds (i.e., large spacing) because this would limit the control range of the flaps/gear when tuning is required later during the approach due to sudden environment changes, uncertainties or prediction errors. As mentioned earlier, it is preferred to save the maximum amount of control authority for the last flap settings. The amount of loss of control authority completely depends on how slow the predecessor executes its approach.

The coarse and fine-tuning processes follow the search strategy described in Sec. III.A. First, flap speeds are altered roughly to their limits until minimum predicted spacing passes over one of the boundaries of the desired spacing margin. Next, if necessary, the previously shifted flap is fine-tuned to get spacing within the margin.

F. Noise and Traffic Optimization

As soon as the aircraft passes the calculated thrust cutback altitude, or the pilot sets thrust to idle above h_{TCB}, the noise and traffic optimization routine is activated. NT optimization continues until the aircraft passes the altitude of the reference height plus 200 ft to avoid late changes of the last flap speed(s).

1. Optimization Constraints

The NT algorithm first determines the own trajectory using the last updated flap schedule and predicts the minimum spacing. If all constraints are still met, no changes to the flap schedule are necessary and the algorithm stops the current loop. The NT optimization constraints are the following:

1) *Spacing goal*: predicted spacing must be larger than minimum safe spacing. If not, flap/gear speeds must be risen.

2) *Noise goal*: the aircraft must reach V_{APP} at the reference height of 1000 ft. This constraint is included in the algorithm by checking the difference Δh between h_{APP} and the predicted altitude where the aircraft reaches V_{APP} (see Fig. 10). When Δh is positive, the aircraft is flying too slow and flap/gear speeds must be lowered. A negative Δh indicates that the aircraft is too fast, so that flaps have to be extended earlier. A tuning margin for Δh of ± 5 ft is taken, because the altitude corresponding to V_{APP} can only be predicted with an accuracy of maximum 10 ft. Presented examples in Fig. 10 show 1) a positive Δh caused by an early thrust cutback (TCB) and 2) a negative Δh resulting from a late extension of flaps 15 deg.

The spacing goal always has priority over the noise goal because safety prevails. If one of the constraints is violated, the binary search algorithm looks for a satisficing flap schedule.

2. Flap Optimization Process

The flap scheduling process has a coarse and fine-tuning cycle, as discussed in Sec. III.A. Flap speeds are increased when spacing is in danger OR Δh is negative (<5 ft). Flap speeds are decreased when Δh is positive (>5 ft) AND spacing is not a problem. After each flap speed change, the trajectory is recalculated. If tuning for spacing, the

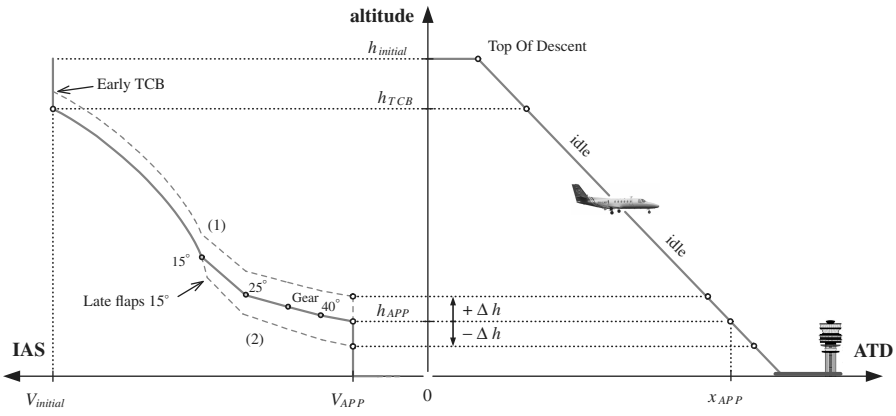

Fig. 10 Predicted position and speed trajectory with a predicted deviation Δh with respect to h_{APP}.

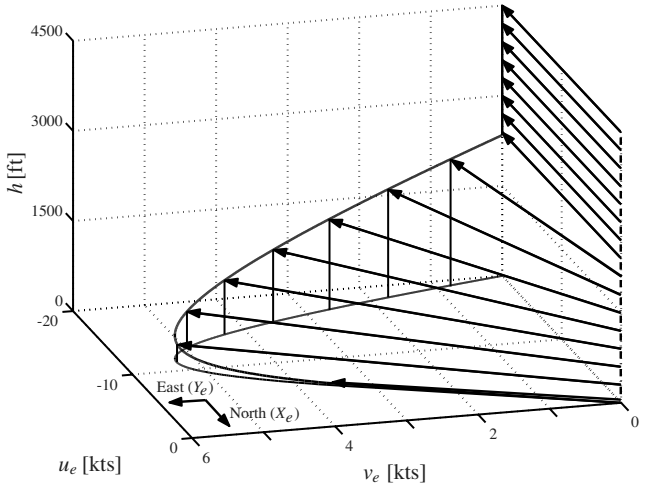

Fig. 11 Logarithmic, rotating wind model; direction 360, speed 20 kn in the free atmosphere.

algorithm increases flap speeds to slowdown faster. Hence, thrust will be applied before reaching h_{APP} (Δh is positive). The algorithm is aware of this and will try to reduce the duration of applying thrust to a minimum. This is achieved by scheduling the own aircraft as close as possible behind the lead, within the $+0.05/+0.1$ NM spacing margin.

IV. Experiment 1: Monte Carlo Simulations

Experiment 1 focused on analyzing performance of the flap scheduler for various wind and traffic scenarios and demonstrating its consistency during repeated runs. It was also an attempt to identify the sensitivity of the algorithm to inaccuracies in the wind prediction and the approximated characteristics of the own aircraft that are incorporated in the trajectory predictor.

A. Method

To validate the TDDA flap scheduling algorithm performance, multiple test scenarios were evaluated with Monte Carlo simulations. Each of these scenarios were repeated 100 times for random turbulence conditions and varying pilot reaction times to get sufficient statistical data.

1. Experiment Design

The Monte Carlo simulations of the TDDA procedure were conducted offline with a 6-DOF nonlinear model of a Cessna C500 Citation I [24]. The aircraft model was augmented with an extra control variable: an additional flap setting at flaps 25 deg. The approach was initiated at 7000 ft with 250 kn IAS, established on the ILS localizer (runway 36) before the glide slope interception point. The autopilot controlled the entire approach, disengaging the autothrottle at h_{TCB}, extending flaps and gear at the calculated speeds, and reengaging the autothrottle when V_{APP} was reached to hold this velocity. V_{APP} was set at 110 kn IAS and h_{APP} was set at 1000 ft.

Another Cessna Citation I performing a TDDA was selected as the leading aircraft and was initially 7.5 NM in front of the own aircraft. Its trajectory took the governing winds into account. The wind profiles were defined according to a time-invariant, rotating, logarithmic wind model [19,25] demonstrating a so-called backing and veering effect of the wind vector as illustrated in Fig. 11. Wind prediction of the flap algorithm was taken identical to the actual wind profile, disregarding turbulence.

The Monte Carlo experiment was divided in two parts. First, general performance was evaluated following a complete test matrix. Second, errors were introduced in the algorithm to explore its robustness.

2. General Performance Analysis: Independent Variables

Three independent variables were varied as listed in Table 1, resulting in 36 scenarios. First, three *levels of optimization* were investigated: 1) the baseline scenario, which uses a fixed "standard" flap/gear deflection scheme, only calculates h_{TCB} to comply with the governing predicted wind; 2) noise-only optimization (NO), where spacing is not taken into account; and 3) NT, which includes the spacing goal as well.

Second, two *lead aircraft approach characteristics*: 1) a "nominal" approach, determined using the standard flap/gear schedule, and 2) a slow approach where the leading aircraft decelerates early because of early pilot deceleration actions. (A slow lead aircraft was referred to as a "fastman" in earlier work [18–21].)

Finally, six *wind conditions*: 1) zero-wind scenario; 2) and 3) head wind conditions of 20 and 40 kn, respectively; 4) 60 kn crosswind coming from a 45 deg direction with respect to the approach path; 5) 40 kn pure crosswind; and 6) tailwind of 20 kn.

3. Robustness Analysis

To evaluate the robustness in flap scheduler performance the following deviations were analyzed: 1) error between the actual and predicted wind profile, 2) error in predicted aircraft mass, and 3) error in approximated drag polar of Eq. (5). Only scenarios with a slow leader are interpreted. Naturally, this traffic scenario is of more interest as it demands more optimization effort.

4. Random Disturbances

Two random disturbances made each run of the Monte Carlo simulation unique. The first variation is turbulence, based on Dryden spectra with additional arbitrary "patchy" characteristics which introduces low-frequency gusts [26]. Second, pilot response times to the thrust cutback, flap and gear cues were varied according to a Poisson probability distribution with a mean time delay of 1.75 s. The distribution was truncated at 5 s, hereby defining the maximum delay.

5. Dependent Measures

The performance of the TDDA procedure was evaluated in terms of 1) the altitude at which V_{APP} is reached ($h@V_{\text{APP}}$) as a *measure for noise impact* (as defined earlier, a deviation in noise performance could either be an undesirable noise impact, or a too late stabilization in the final approach configuration), and 2) the minimum actual

Table 1 The Monte Carlo experiment matrix of 36 test scenarios, formed with three independent variables, that is, level of optimization, lead approach characteristic, and wind condition

Optimization level	Lead trace type	Wind condition[a]					
		360/00	360/20	360/40	045/60	090/40	180/20
Baseline	Nominal	1	2	3	4	5	6
	Slow	7	8	9	10	11	12
Noise only	Nominal	13	14	15	16	17	18
	Slow	19	20	21	22	23	24
Noise and traffic	Nominal	25	26	27	28	29	30
	Slow	31	32	33	34	35	36

[a]Wind notation *xxx*/*yy* indicates wind coming from a relative angle *xxx* with a speed *yy* in kn.

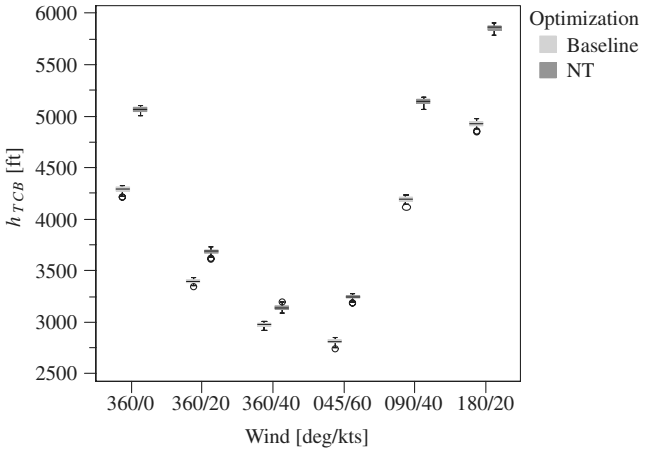

Fig. 12 Thrust cutback altitudes in case of a "slow" lead trace.

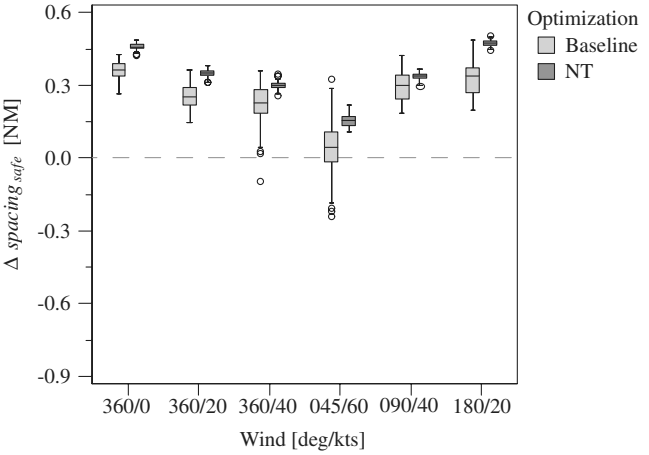

Fig. 13 Deviation from 2.5 NM safe separation for a nominal lead type under all wind conditions.

distance with respect to the 2.5 NM safe spacing ($\Delta\text{spacing}_{\text{safe}}$) as a *measure for spacing performance*. A full-factorial model analysis of variance (ANOVA) was conducted to evaluate the effects of the independent measures on these performance indicators. Boxplots (Fig. 12) were created to visualize the center and spread of the results. The boxplots also reveal outliers in the data that are presented in the plots with a circle. These outliers are extreme deviations and were mainly caused by immediate or very late cue responses, possibly in combination with high gust peaks.

B. Results and Discussion: General Performance Analysis

1. *Spacing Goal*

The deviations from the minimum safe separation of 2.5 NM encountered throughout the entire approach are shown in Figs. 13 and 14. As observed, a slow lead reduces the relative spacing significantly, depending on the governing wind. This yields large violations of safe spacing for the baseline and NO optimization level. Adding traffic optimization clearly gives the algorithm a good consistent performance for all wind conditions, where spacing is *never violated*. The effect of optimization for a slow lead type is highly significant ($F_{2,1782} = 20319.946,\ p < 0.001$). Also for a nominal lead, the optimization level has a highly significant influence on minimum spacing ($F_{2,1782} = 836.442,\ p < 0.001$).

The significant performance improvement achieved with NT scheduling originates from the thrust cutback altitude optimization. To comply with both noise and spacing goals as well as possible, thrust cutback (TCB) heights are raised as presented in Fig. 12. A positive outcome is the lower noise production, which is penalized, however, with a reduced downward control authority of the flaps and gear because the margin with respect to its lower speed boundary decreases.

A small excess in final spacing can be observed and is caused by the limited accuracy of the lead trajectory prediction during the initial part of the approach (second order fit, Fig. 5). The form of the lead aircraft deceleration characteristic primarily affects the performance of the spacing prediction. The exact deceleration rate of the lead depends on both the governing wind and the lead's behavior type. These two independent variables significantly interact with each other to get the resulting actual minimum spacing ($F_{5,1188} = 17349.046,\ p < 0.001$ for NO optimization). Notice also that the lead aircraft type has an influence. Thus, the actual spacing trend is highly variable and therefore hard to predict accurately most of the time. Increasing the spacing prediction algorithm accuracy is expected to be a challenging quest.

2. *Noise Goal*

As expected and shown in Figs. 15 and 16, $h@V_{\text{APP}}$ lies consistently closer to the target of 1000 ft when the algorithm schedules the flaps and gear accordingly ($F_{2,1782} = 1944.213,\ p < 0.001$ and $F_{2,1782} = 334.689,\ p < 0.001$, for, respectively, the nominal and slow lead). A post hoc analysis on the optimization level

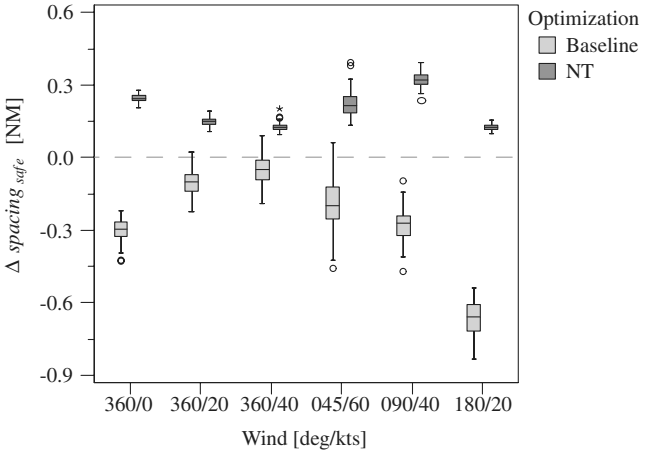

Fig. 14 Deviation from 2.5 NM safe separation for a slow lead type under all wind conditions.

(Student–Newman–Keuls, $p = 0.05$) reveals that the difference between baseline and optimization is indeed significant. On the other hand, the mutual difference between the two algorithm levels (NO and NT) is not significant. (A thorough comparison of both algorithm levels is presented in De Prins et al. [19].) And so, the algorithm can reach similar performance with respect to noise for all headwind type conditions, independent of the fact that spacing was predicted to be safe or not. Lead type has no significant influence on $h@V_{\text{APP}}$ ($F_{2,1782} = 0.273,\ p = 0.601$). Hence, noise and spacing goals can be readily combined.

For the tailwind scenario 180/20, some noise abatement has to be sacrificed to keep a safe spacing behind the slow lead. The algorithm had to come up with a h_{TCB} of almost 6000 ft to solve the loss of spacing (Fig. 12). Consequently, the spacing prediction algorithm has less lead data points to accurately generate the spacing trend before TCB. The lack of data points, in combination with the effect of tailwind on the form of the lead's trajectory, results in an overestimation of spacing.

Finally, the two-dimensional own trajectory prediction with the point mass model proves to have good performance for every three-dimensional wind profile. Although ANOVA indicates that the wind has a highly significant effect on the target altitude when both optimization levels are applied ($F_{5,1188} = 316.706,\ p < 0.001$), the absolute mutual differences are only very small.

3. *Conclusions on General Performance*

It can be concluded that the TDDA algorithm is able to adequately combine the noise and spacing goals in most scenarios. With respect to traffic, the support system *always* assures a consistent, safe

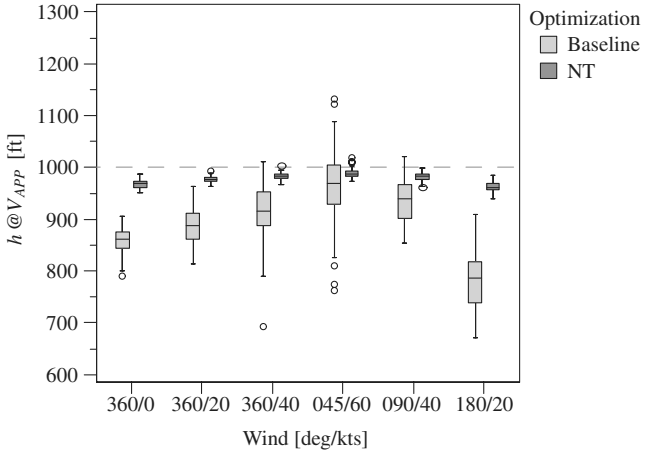

Fig. 15 Altitude at which V_{APP} is reached for a nominal lead type under all wind conditions.

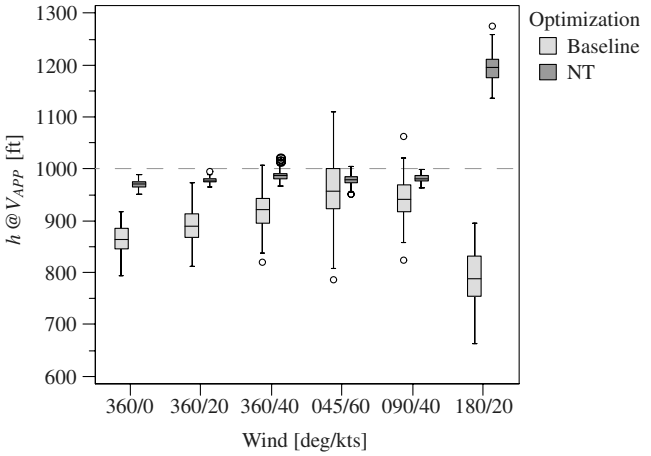

Fig. 16 Altitude at which V_{APP} is reached for a slow lead type under all wind conditions.

approach in any wind condition for a nominal and slow lead. A satisfying accuracy for h_{APP} was found in the order of 0 to 40 ft, independent of the lead deceleration characteristic. (An important note is that an exact wind prediction has been used for the above analysis. Wind prediction offsets are investigated in the following robustness analysis. A further analysis on wind errors and a comparison of the logarithmic wind profile prediction and a statistical based wind estimator for the TDDA algorithm has been described by de Gaay Fortman et al. [20].)

C. Results and Discussion: Robustness Analysis

1. *Sensitivity to Wind Prediction Errors*

The predicted wind velocity in the free atmosphere was offset with ± 10 kn and ± 20 kn for the 360/40 headwind, and ± 10 kn for the 045/60 side wind. Figure 17a presents the spacing achievements. Overestimation of the wind naturally has a negative effect on spacing due to the later TCB. Still, NT optimization has no problem to ensure safe spacing, even for an error of 20 kn. The algorithm also attains a relatively good precision in target altitude (Fig. 17b). When underrating wind, $h@V_{APP}$ increases because the aircraft decelerates faster than expected. Notice that even better results are achieved than without the wind error (Fig. 16) due to some compensation by the last tardy flap selection. Predicting more head wind reduces the accuracy slightly by approximately 20 ft per 10 kn error. Adapting the approach for slow traffic is handled nicely by the NT algorithm without the need to add thrust too early.

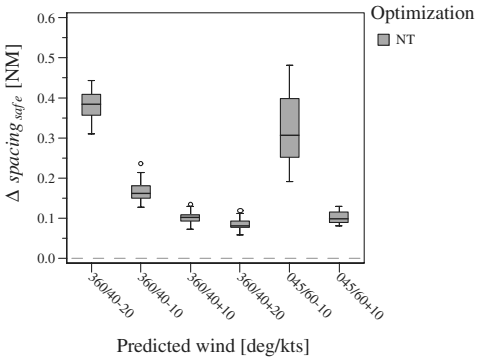

a) Deviation from 2.5 NM safe separation

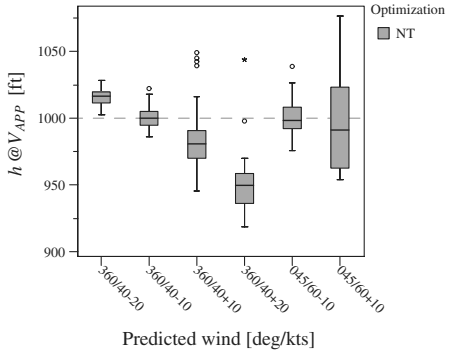

b) Altitude at which V_{APP} is reached

Fig. 17 Robustness performance for a slow lead and wind prediction error of ±10 kn and ±20 kn.

2. *Sensitivity to Mass Prediction Errors*

A 10% mass error has been evaluated with respect to the standard 5000 kg weight of the Citation I, that is, a predicted mass of 4500 and 5500 kg. Predicting 10% lower mass decreases h_{TCB} significantly (the along-track gravity force component is smaller) and consequently has a detrimental impact on minimum spacing (Fig. 18a). Nevertheless, NT optimization is still able to correct the lack of spacing to 2.6 NM. This is achieved at the cost of noise impact because thrust is reapplied earlier, see Fig. 18b. Still, the algorithm can bring the target altitude relatively close to 1000 ft. The 5500 kg prediction eases the traffic situation and realizes a better target altitude than with the exact mass because it compensates for the cue delays.

3. *Sensitivity to Drag Polar Errors*

Finally, errors were applied to the predicted drag polar by offsetting the $C_L - C_D$ curve sideways: Eq. (5) has been augmented with gains of ± 5 and $\pm 10\%$. A higher predicted drag naturally lowers h_{TCB} and decreases minimum spacing (Fig. 19a). The algorithm is once more capable of resolving the traffic conflict. Figure 19b shows that safe spacing in the $C_D + 10\%$ scenario can only be guaranteed by arriving at V_{APP} up to 200 ft above the desired h_{APP}. Considering the amount of drag error and slower lead, this is still a limited reduction in noise performance. For the other scenarios, an (obvious) later stabilization can be seen where drag is overvalued and a small noise penalty when underrating drag. An absolute target altitude deviation of 50 to 100 ft for, respectively, the 5 and 10% mismatch of C_D is still acceptable.

4. *Conclusions on Algorithm Robustness*

The sensitivity analysis reveals that the flap/gear scheduling algorithm can cope with errors in wind, mass, and drag prediction quite well. The spacing goal is *always* achieved, whereas the noise performance is only slightly declined. A comparison of all the results indicates that the optimization algorithm is most sensitive to

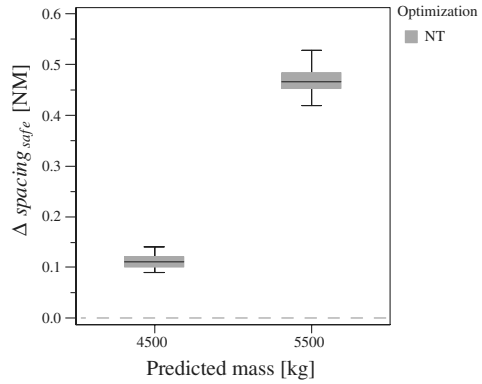

a) Deviation from 2.5 NM safe separation

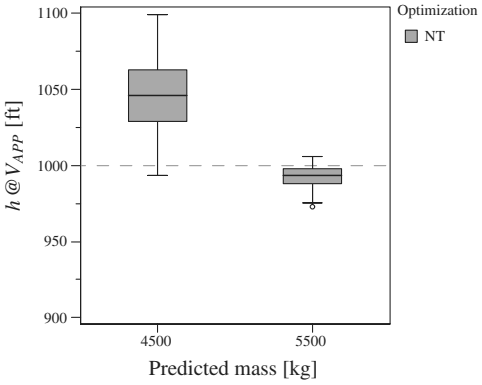

b) Altitude at which V_{APP} is reached

Fig. 18 Robustness performance for a slow lead in zero-wind and aircraft mass error of ±500 kg.

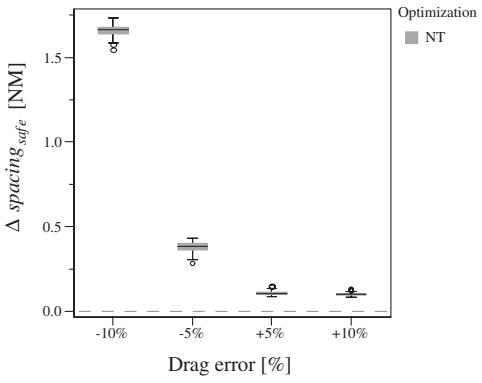

a) Deviation from 2.5 NM safe separation

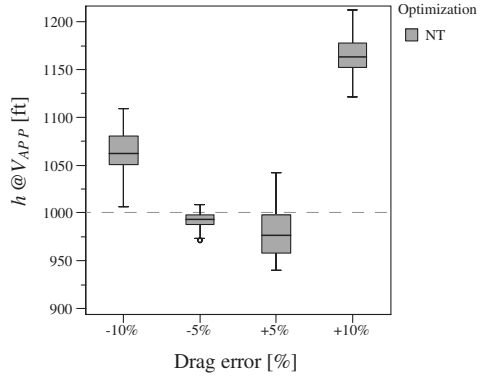

b) Altitude at which V_{APP} is reached

Fig. 19 Robustness results for a slow lead in zero-wind and drag coefficient error of ±5 and ±10%.

mismatches in the drag polar. However, drag and lift information can be determined rather accurately with sufficient flight test data [21]. It should be possible to calculate aircraft mass at takeoff and fuel consumption with an error of less than 10% of the total weight. Therefore, the highest expected error during TDDA operations is most likely a mismatch between the predicted and actual wind profiles.

V. Experiment 2: In-Flight Investigation

Experiment 2 was the first attempt to evaluate the feasibility of self-spacing during continuous decelerating approaches in real flight. The experiment also complements the Monte Carlo studies, especially in support of the robustness characteristics of the scheduling algorithm. The flight tests, conducted in February 2005 at Soesterberg military airport, included one test flight and one actual exploratory flight with multiple approaches [21]. Only the results of the experiment addressing the algorithm performance will be described.

A. Method

1. *Apparatus: Aircraft and TDDA Display*

The Cessna C550 Citation II laboratory aircraft of Delft Aerospace, a light twin-engine corporate jet, was used in the test flight. The aircraft has standard three flap settings (flaps UP, 15 and 40 deg). As for the Monte Carlo simulations, a new flap setting was indicated in the cockpit, namely flaps 25 deg, to increase the control range of the approach procedure. The TDDA interface of Fig. 2 was presented on a 15 in. LCD screen that was mounted in front of the copilot's seat. The aircraft was equipped with a flight test instrumentation system, developed in-house, that gathers the aircraft data from the onboard flight management system, air data computer and own sensors, and publishes this information to a distributed double laptop setup which ran the TDDA software.

2. *Procedure and Instructions to Subjects*

All approaches were performed by one pilot (age 29; 250 h on C550) that was extensively briefed before the flights. During the TDDA, the right pilot was the pilot flying (PF), whereas the left pilot (captain) acted as a safety pilot. Before the start of the TDDA procedure, the captain brought the aircraft with the aid of the autopilot to level flight at 5000 ft, at 230 kn IAS, and fully established on the localizer interception of Soesterberg's active runway 27. Meanwhile, the experiment controller, sitting in the back, initiated and started the new experiment run on the laptops. The initialization included the generation of a "virtual" lead aircraft, based on a simple aerodynamic model of a Cessna Citation I and the current meteorological conditions. The PF then disconnected the automation aids and flew the TDDA procedure with the aid of the flight director. The pilot was instructed to strictly adhere to the flap/gear and thrust cutback cues, so that the performance of the algorithm could be fully assessed in real flight. The safety pilot was asked to deploy flaps and gear on the PF's command and to communicate with ATC. Each successful approach was aborted at an altitude of approximately 800 ft, after which the captain returned the aircraft to the experiment start position. In every approach the governing wind profile was recorded and used during the next approach as a persistent wind prediction for the flap algorithm and lead aircraft trajectory generation.

3. *Data Acquisition and Processing*

Most aircraft parameters were retrieved directly from the aircraft. Two important variables, flap position and landing gear position, could not be acquired and had to be manually incorporated by the experiment controller, triggered by the pilot's flap/gear callout. Wind direction and speed were calculated by comparing the available ground and airspeed vectors. ILS localizer/glide slope, together with flight director signals, were computer generated using global positioning system data, as glide slope signals cannot be intercepted during the initial part of a straight-in approach from 5000 ft.

Table 2 Review of experiment flight results. The table presents the different scenarios along with the calculated thrust cutback (TCB) altitude, time differences between cue presentation and actual flap/gear selection, as well as the altitude at V_{APP} (120 kn) and the minimum spacing with the predecessor during the approach[a,b]

Run	Lead type	TCB, ft	Δt F15, s	Δt F25, s	Δt F40, s	Δt LG, s	h at V_{APP}, ft	Min. spacing, NM
1)	Nominal	3550	2.9	−1.9	0.6	0.8	760[c]	4.0
2)	Nominal	3520	−1.9	7.3	5.9	0.8	917	4.4
3)	Slow (7.5 NM)	3410	——[d]	——[d]	1.0	0.5	953	3.6
4)	Slow (7.5 NM)	3200	−0.7	2.1	1.3	1.8	1012	3.5
5)	Slow (6.0 NM)	3280	1.6	1.0	3.4	3.1	955	2.7
6)	Slow (5.5 NM)	3850	2.0	2.1	−0.5	−7.3	914	2.7

[a]F15: flaps 15 deg; F25: flaps 25 deg; F40: flaps 40 deg; LG: landing gear.
[b]$\Delta t > 0$ indicates too-late flap/gear selection.
[c]Thrust was added already at 1060 ft while V_{APP} was not yet reached. Extrapolation of the deceleration rate suggests an adequate target performance.
[d]Unreliable data in this part of the logged data file.

B. Results and Discussion

In Table 2, all data of interest for the flight test are summarized. A total of six consecutive approaches were performed in which the initial spacing with the lead aircraft was gradually decreased to call in traffic scheduling. As a result of the slower lead aircraft, the algorithm selected a higher h_{TCB} to ensure conflict resolution. The pilot showed a strict adherence to the flap/gear cues. The average delay between cue presentation and actual flap/gear selection was measured to be 1.17 s. A few anomalies in cue follow-up occurred (runs 2 and 6), caused by misinterpretation between pilot and experiment controller, pilot anticipation to the cues, and ATC communication interferences.

In all approaches the minimum required spacing of 2.5 NM was never violated, even with a very slow lead aircraft in front (run 6). The target speed V_{APP} was always reached below the target altitude of 1066 ft [1000 ft plus field elevation (66 ft)] and averaged 950 ft. The lower target altitudes were mainly caused by delays in flap/gear selection and deviations from the 3 deg ILS glide path once the algorithm stops scheduling the lasts flaps within 200 ft of the target altitude [19].

The results show that, with the current algorithm and using persistent wind data, it is possible to perform a TDDA with a small jet aircraft and simulated traffic while achieving the noise *and* spacing goals. Figure 20 illustrates the flap and gear behavior, wind information (headwind is negative), and the spacing with the predecessor for run 4. The course of the flap and gear cues indicates a gentle tuning process that oscillates near the nominal speeds. Upper and lower speed boundaries are avoided.

C. Conclusions of the In-Flight Experiment

The flight tests were the first to investigate the viability of self-spacing during decelerating approaches in real flight. The results are well in line with the previously conducted Monte Carlo experiments and prove that it is possible to perform a TDDA in real life with the current algorithm and persistence wind data. All approaches showed a consistent target performance in terms of reaching V_{APP} at the prespecified altitude, whereas simultaneously the algorithm managed to take care of spacing with simulated traffic in front when necessary.

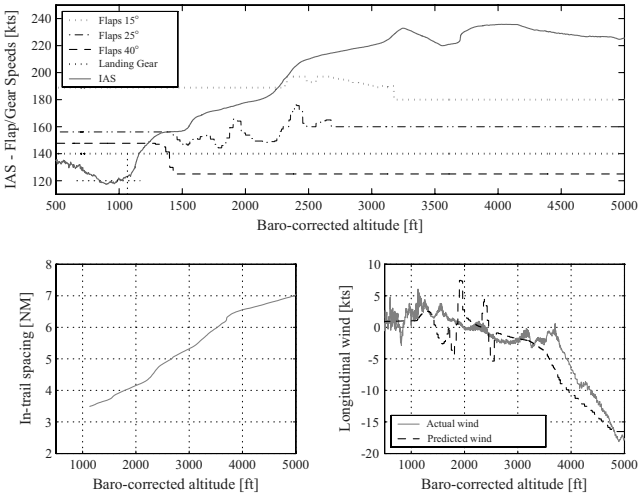

Fig. 20 Flap/gear behavior, spacing trend, and longitudinal wind component for in-flight run 4.

VI. Experiment 3: Piloted Simulator Tests

Experiment 3 complemented the previous studies by evaluating operational performance when pilots manually fly a TDDA aided by the automated tool. Its additional focus was to determine whether pilots would do equally well without assistance of the algorithm, and to quantify pilot workload.

A. Method

1. Apparatus

The SIMONA Research Simulator, the 6-DOF motion research flight simulator of Delft University,[**]was used for the experiment. All approaches were performed at runway 27 of Schiphol Airport (EHAM). Aircraft control was provided via a wheel/column combination (with trim button) and rudder pedals. Flap selector, gear handle, and throttle levers were positioned on the right-hand side of the captain's seat. Real jet aircraft sound, coupled on throttle setting, was played during the experiment runs.

2. Aircraft Model and Atmospheric Disturbances

The aircraft flown was a nonlinear 6 degree-of-freedom Cessna C500 Citation I mathematical model [24], as before augmented with the extra flap setting of 25 deg. Wind was simulated by replaying a data file containing prerecorded wind observations partitioned into altitude intervals of 500 ft (Fig. 21). Similar to the in-flight investigation, persistent wind data (10 min old) were used to predict the own trajectory. Atmospheric turbulence was considered to be a stationary stochastic process based on Dryden spectra with patchy behavior [26].

3. Independent Variables

The following three independent variables were varied throughout the experiment: 1) level of automation and display type, 2) deceleration characteristics of the lead aircraft, and 3) wind type.

a. Level of Automation and Display Type. Two levels of automation were applied in the experiment. First, the TDDA procedure was performed with *no automation* (baseline), that is, the pilot was required to schedule thrust cutback, flaps, and gear at his own discretion to achieve the noise goal and/or spacing goal. The pilot was supported only by an approach plate with indications on thrust cutback altitude and flap/gear timing for a zero wind condition. On the ND, only the actual position of the lead aircraft was presented. In this way, the pilot was left with only the information available in the cockpit nowadays. Second, *NT scheduling* was enabled. In this case, the pilot was supported by a full display (Fig. 2), with flap/gear

[**]Simona Web site, http://www.simona.tudelft.nl [cited 1 July 2006].

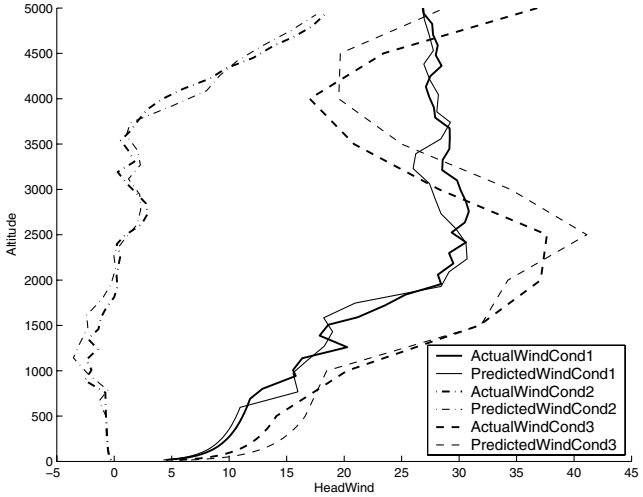

Fig. 21 Predicted and actual wind speed profiles during the simulation experiments. A positive value indicates headwind.

cues, TCB cue, thrust/drag annunciators, and spacing arc information. The baseline approach serves as a threshold for data and workload analysis.

b. Lead Characteristics. Two different lead trajectories have been evaluated: 1) a nominal lead, which follows the same (fixed) common-procedure flap schedule, and 2) a slow lead, which decelerates earlier resulting in a spacing violation if no action is taken. In all cases, the preceding aircraft was a Cessna Citation I that executed the standard TDDA procedure, initially spaced 7.5 NM with the own aircraft. Both aircraft had an identical V_{APP} and h_{APP}, that is, 110 kn and 1000 ft, respectively.

c. Wind. Three wind conditions were defined (Table 3): two conditions that were recorded during the flights with the Cessna Citation II laboratory aircraft (W1, W2), and one crosswind condition of 50 kn with a direction of approximately 45 deg with respect to the approach path (W3).

4. Experimental Design and Procedure

A full-factorial within-subjects design was applied, yielding the 12 conditions ($2 \times 2 \times 3$) of the experiment matrix of Table 4. The scenarios were randomized for every pilot. Each subject first conducted training sessions in which each lead type and automation level was encountered at least once. When familiarized with the procedure, each pilot completed every experimental condition once (12 runs).

Each approach scenario started at level flight at 5000 ft, 230 kn IAS, with the aircraft fully established on the localizer of runway 27 before the ILS glide slope interception. Before the start of each run, the pilots were informed about the wind speed and direction yielding at the ground and start altitude. Flight path control occurred manually, assisted by the flight director signals. The approach speed V_{APP}, set at 110 kn IAS, had to be achieved at a reference altitude of 1000 ft. Minimum safe separation was fixed at 2.5 NM. A single approach lasted approximately 6 min.

A single pilot was used for data collection, with an experiment controller in the right seat. The copilot solely selected the appropriate flaps and gear position on the pilot's callout. The two-person arrangement provided the opportunity to collect data and investigate pilot workload, while still preserving the realism of multicrew tasks.

Table 3 Experiment wind information

	0 ft	5000 ft
Wind condition 1 (W1)	220/10	240/30
Wind condition 2 (W2)	160/1	290/20
Wind condition 3 (W3)	300/8	310/50

Table 4 Experiment matrix for the piloted simulator tests

	Wind condition 1 (W1)		Wind condition 2 (W2)		Wind condition 3 (W3)	
	Nominal	Slow	Nominal	Slow	Nominal	Slow
Baseline	1	2	3	4	5	6
NT algorithm	7	8	9	10	11	12

After each subsequent run, pilots were asked to fill in the NASA task load index (TLX) [27] which is used to assess pilot workload. In addition, a postexperiment questionnaire was administered after the completion of all runs. The questionnaire invited pilots to give their opinion on several topics, such as display/algorithm properties, lead aircraft behavior, workload, situational awareness, simulation properties, etc.

5. Subjects and Instructions to Subjects

In total, ten qualified captains and first officers participated in the experiment [21]. Most of them had previous experience with noise abatement procedures. The mean age and flight time of the pilots was 43.4 years and 10,830 hours, respectively. Before the experiment, pilots were briefed about the TDDA procedure, the objective of the experiment and characteristics that may influence the outcome. All pilots were instructed to perform the TDDA procedure manually as accurately as possible, with the engines running completely at idle. They were commanded to maintain 230 kn IAS until thrust cutback. Then, the throttle levers had to be placed to their idle detent position. During the approach, the pilots had to minimize deviations from the 3 deg glide path and flap/gear cue advisories. At all times, the aircraft had to be fully configured (full flaps and landing gear down) by the time that it reached an altitude of 1000 ft. Furthermore, the pilots were instructed that, at no time, the in-trail spacing should be less than 2.5 NM. In addition, the power levers should not be moved from their idle position apart from when thrust is required to maintain V_{APP}.

6. Dependent Measures

Operational performance was reviewed by means of $h@V_{APP}$ and $\Delta\text{spacing}_{safe}$. Pilot performance was evaluated by recording flap/gear activities and the time delay between flap/gear cue presentation and pilot response. Pilot workload was judged using the TLX.

7. Experiment Hypotheses

It was hypothesized that pilots would achieve better operational performance when they were assisted by the automation. Especially in the cases of a slow lead aircraft, the automation should outperform the unassisted pilot. With the aid of the scheduler, it was hypothesized that V_{APP} would be reached at h_{APP} more consistently and in full landing configuration, while keeping safe spacing. In addition, it was hypothesized that stronger winds would deteriorate the pilot's ability to achieve V_{APP} at h_{APP}, whereas this effect would be less pronounced when assisted by automation. Another hypothesis was that the automation and accompanying interface would decrease workload as compared with the baseline.

B. Results

1. Operational Performance

a. Noise Goal. For the "slow lead" baseline approaches (Fig. 22), pilots were typically not capable of reaching V_{APP} at h_{APP}, except for the "easier" wind condition 2. However, in the latter wind scenario, most pilots seriously violated safe spacing (Fig. 23b). A nominal lead behavior yielded a significant better target altitude accuracy ($F_{1,9} = 9.366,\ p = 0.014$). Stronger winds significantly deteriorated the baseline performance with a slow lead ($F_{2,18} = 7.072,\ p < 0.001$), however, no statistically significant difference could be found with the nominal lead ($F_{2,18} = 2.533$, $p = 0.107$).

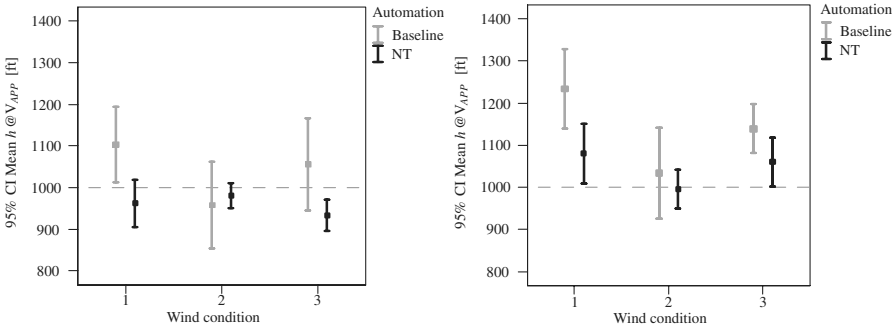

a) Nominal lead aircraft b) Slow lead aircraft

Fig. 22 The means and 95% confidence intervals of the altitude at which V_{APP} was reached.

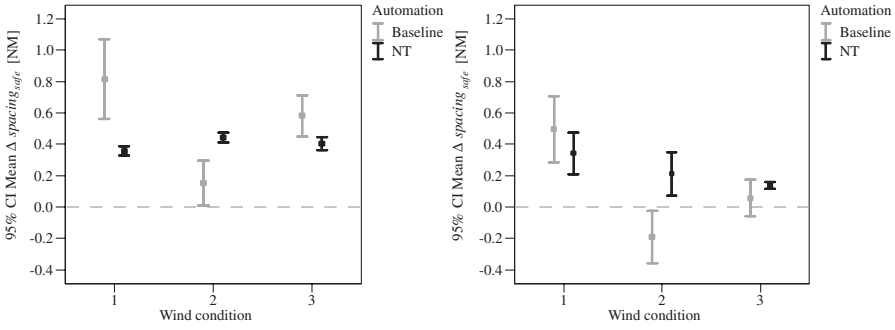

a) Nominal lead aircraft b) Slow lead aircraft

Fig. 23 The means and 95% confidence intervals of the deviations from minimum safe spacing.

When presented with the automation and supporting display, pilots were capable of reaching the target altitude more consistently, expressed in the lower variability and means closer to the target altitude (nominal lead: $F_{1,9} = 10.512$, $p = 0.010$; slow lead: $F_{1,9} = 8.668$, $p = 0.016$). Because the algorithm will always prioritize on safe spacing, a slower lead aircraft evidently decreases the noise reduction performance with the automation ($F_{1,9} = 26.059$, $p = 0.001$). Wind, however, showed no significant influence ($F_{2,18} = 2.504$, $p = 0.110$).

b. Spacing Goal. Figure 23 illustrates the deviations from the minimum safe spacing of 2.5 NM throughout the whole approach. As hypothesized, safe spacing distinctly decreased with a slower lead aircraft when pilots are not assisted ($F_{1,9} = 84.125$, $p < 0.001$). They only managed to cope with a slow lead in the first wind scenario; however, this was accompanied by a detrimental effect on $h@V_{APP}$ (Fig. 22b). Actually, the more the pilots tried to achieve V_{APP} at the target altitude, the more they exceeded or tended to exceed the safe spacing threshold. The wind characteristics also significantly influenced spacing performance ($F_{2,18} = 23.600$, $p < 0.001$).

When the automation was used, the variance in performance reduced considerably for both the normal and slow predecessor (W1: $F_{1,9} = 16.552$, $p = 0.003$; W2: $F_{1,9} = 21.288$, $p = 0.001$; W3: $F_{1,9} = 11.684$, $p = 0.008$). Accordingly, as in the baseline, $\Delta\text{spacing}_{safe}$ becomes much smaller for a slow lead with respect to a normal predecessor ($F_{1,9} = 32.790$, $p < 0.001$).

The most important contribution of the automation is that safe spacing is never violated. In fact, the automation is able to "close the gap" in comparison with the baseline. An ANOVA analysis revealed that automation had a borderline significant effect on deviating from 2.5 NM spacing with a slow lead ($F_{1,9} = 4.345$, $p = 0.067$), where the effect is highly significant for wind condition 2 ($F_{1,9} = 12.602$, $p = 0.006$).

2. Pilot Controls

To be fully configured, a total of three flap and one gear activities had to be performed. When assisted by the automation, the pilot was able to be fully configured at the end of the TDDA, although this was certainly not always the case for a baseline approach in the more "severe" wind conditions. Wind and automation proved to have a (borderline) significant effect on achieving full configuration (respectively, $F_{2,18} = 3.273$, $p = 0.061$ and $F_{1,9} = 3.578$, $p = 0.091$). Choosing a too-early thrust cutback forced the pilots to delay flap and gear extension to extend the glide. In some cases, this resulted in not selecting the last flap or gear before V_{APP} was reached. No significant differences were discovered due to lead behavior ($F_{1,9} = 2.250$, $p = 0.168$).

The pilot response time on the flap and gear cues demonstrated a trend toward anticipation of the flap and gear cues when confronted with a sluggish predecessor (Fig. 24). Indeed, the effect of lead characteristics type was significant ($F_{1,9} = 9.270$, $p = 0.014$). Pilots were less rigorous in following the thrust cutback cue (Fig. 25). They mostly awaited the thrust cutback cue, and sometimes completely missed them.

3. Workload and Post-Test Questionnaire

The workload ratings in Fig. 26 show a highly significant decrease in workload with the aid of the automation and display as hypothesized ($F_{1,9} = 107.622$, $p < 0.001$). No significant differences were found for the wind condition ($F_{2,18} = 2.131$, $p = 0.148$).

Pilot comments and subjective ratings given in the questionnaire indicate that the automation was indeed a helpful tool to execute a TDDA, and brought instrument scan, workload, and situational awareness to a level comparable to current ILS approaches.

C. Conclusions of the Simulator Trials

For the tested wind conditions, it can be concluded that when pilots have to time thrust cutback, flap, and gear selection on their own, they are able to reach V_{APP} at the projected altitude when a nominal lead is in front. However, pilot performance deteriorates significantly with more sluggish lead aircraft, either by reapplying thrust too early to maintain V_{APP} or by violating minimum safe spacing. A distinctly better and more consistent noise performance is found when optimized cues are presented, while safe spacing from the predecessor is established at all times. Additionally, the

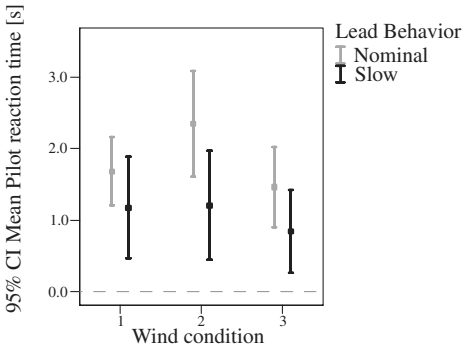

Fig. 24 Means and 95% confidence intervals of pilot response time on flap and gear cues.

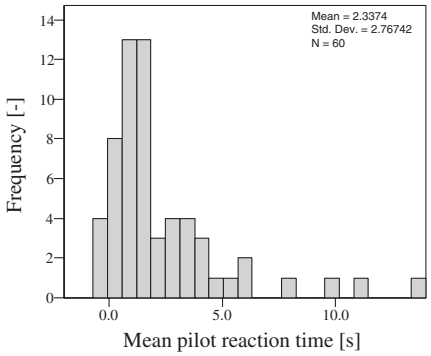

Fig. 25 Histogram of the pilot response time on the thrust cutback cue.

assistance of the algorithm and display clearly decreases pilot workload up to an effort level comparable to current standard approaches. All in all, the pilot support interface and accompanying scheduling algorithm provides an essential tool to perform TDDAs.

VII. Discussion

Given the results presented in the paper, it appears that pairwise self-spacing is feasible when performing a continuous decelerating approach using the designed onboard automation. Hence, the proposed concept might offer a valuable solution to the implementation of noise abatement approach procedures without a major decrease in runway capacity. This hypothesis should be further substantiated with offline simulations on a stream of aircraft with a mixed fleet to quantify runway capacity and identify the potential occurrence of chain reactions of more-and-more earlier decelerating aircraft. Augmenting the flap scheduling algorithm with the capability to decrease spacing is hypothesized to be valuable for gaining capacity. Follow-on work should also focus on the monitoring task reserved for the air traffic controller. A controller-in-the-loop experiment should be conducted to assess the controller's

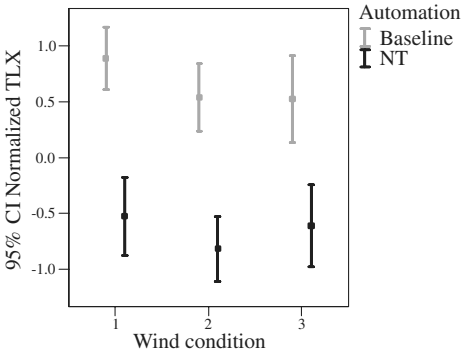

Fig. 26 The means and 95% confidence intervals for the normalized TLX scores.

acceptance of the proposed procedure, analyze the overall system performance, and identify potential bottlenecks. Finally, future work should also explore the application of a near-idle throttle setting to the TDDA, as this would allow for some additional control authority after thrust cutback to possibly improve performance at a modicum of noise and fuel use.

The experiments also showed that accurate trajectory prediction, onboard in this case, but it will apply to ground based as well, strongly relies on an adequate wind estimation. Therefore, a repeated broadcast of the onboard calculated wind velocity and wind direction through some data link network, such as Mode S or ADS-B, is envisioned to be valuable for both scenarios. It is also hypothesized that sharing atmospheric data and aircraft intent will be essential for improving the overall air traffic management system and especially terminal area operations.

This observation also triggers the discussion whether ground-based or air-based systems are most suited for trajectory prediction. The primary advantage of onboard trajectory prediction is that the aircraft onboard systems best know its state, its performance characteristics, the airline preferences, and the way the flight management system operates. Real-time adaptations of the execution of an advanced approach can be easily made when unexpected deviations from the desired trajectory occur; for example, the proposed concept of changing the flap schedule to meet the noise constraints. A primary disadvantage is the considerable investment required to implement new onboard software on current flight decks. Therefore, it is recommended that the potential to easily and at low-cost implement additional functionality into flight management systems is considered when developing or acquiring such a system.

The use of a ground-based system obviates the need for estimation of the trajectory of the preceding aircraft as needed in an air-based system. Investment costs would be more focused, because deployment would be done only at the busiest airports. However, this solution also has some significant disadvantages. First, it would be difficult to incorporate the performance data for the fleet of aircraft arriving at an airport, especially because the level of detail needed is significantly higher than in use for current ground-based aircraft performance databases. Second, this solution would need extensive communication between the aircraft and the ground-based system for exchange of aircraft-related data and for flap setting, gear, and thrust commands. Hence, the proposed concept of a flap scheduling algorithm that is robust to less accurate lead aircraft trajectory predictions is worth continued research.

VIII. Conclusions

The flap scheduling algorithm proved to be valuable in achieving adequate and consistent performance in executing a self-spaced noise abatement procedure, such as the three-degree decelerating approach. The algorithm is able to adequately combine safe spacing with target altitude accuracy for a range of wind and traffic scenarios, while being robust to relatively large prediction errors for wind, aircraft mass and aircraft drag. When aided by the automation, pilot workload was reported to remain similar to the workload level of current standard approach procedures. The exploratory demonstration flight proved that it is feasible to execute a continuous decelerating approach at idle thrust under actual flight conditions, using the current algorithm and persistent wind data, while ensuring safe spacing with a simulated predecessor throughout the whole approach.

Acknowledgments

The authors express their gratitude to the staff of Delft University's Institute for Simulation, Motion and Navigation Technologies, in particular to Olaf Stroosma, for their essential contributions in conducting experiment 3, and to the staff of the Delft University Flight Department for their indispensable efforts in realizing the in-flight experiment 2. The authors also wish to thank all pilots who participated in the two experiments.

References

[1] Wubben, F. J. M., and Busink, J. J., "Environmental Benefits of Continuous Descent Approaches at Schiphol Airport Compared to Conventional Approach Procedures," National Aerospace Laboratory (NLR), Technical Rept. NLR-TP-2000-275, Amsterdam, The Netherlands, 2000.

[2] Anon., "Sourdine D3: Establishment of Noise Abatement Solutions," Technical Rept. SOURDINE/NLR-DOC-D3-001, Amsterdam, The Netherlands, 2000.

[3] Anon., "Sourdine D5: Final Report," Technical Rept. SOURDINE/ISR-DOC-D5-018, Amsterdam, The Netherlands, 2000.

[4] Elmer, K., Wat, J., Shivashankara, B., McGregor, D., and Lambert, D., "A Continuous Descent Approach Study Using Ames B747-400 Flight Simulator," AIAA Paper 2002-5869, 2002, pp. 1–9.

[5] Clarke, J. P., Tan Ho, N., Ren, L., Brown, J. A., Elmer, K. R., Tong, K., and Wat, J. K., "Continuous Descent Approach: Design and Flight Test for Louisville International Airport," *Journal of Aircraft*, Vol. 41, No. 5, 2004, pp. 1054–1066.

[6] Reynolds, T. G., Ren, L., Clarke, J. P., Burke, S. B., and Green, M., "History, Development and Analysis of Noise Abatement Arrival Procedures for UKAirports," AIAA Paper 2005-7395, 2005, pp. 1–11.

[7] Manzi, P., Lindberg, L. G. V., Wichman, K., Bleeker, O., and Langhans, S., "Improving Operational Efficiency in the Airport, Airline and ATM Processes," *Proceedings of the 23rd Digital Avionics Systems Conference*, No. 3.C.6, Vol. 1, IEEE, Piscataway NJ, 2004, pp. 1–11.

[8] Ayache, F., "OPTIMAL Operational Concept Deliverable D1.2," Eurocontrol Experimental Centre (EEC), Technical Rept. WP1.2-EEC-001-V1.0-ED-PU, Brétigny, France, 2005.

[9] Huemer, R. G., Koenig, R., Friehmelt, H., Isermann, U., and Boguhn, O., "The Influence of Modern Noise-Simulation-Tools on the Design of Future Noise-Abatement-Approach-Procedures," AIAA Paper 2004-5242, 2004, pp. 1–12.

[10] Gershzohn, G., Wat, J., Dwyer, J. P., Elmer, K., Clarke, J. P., and Tan Ho, N., "Advanced Noise Abatement Procedures: An Experimental Study of Flight Operational Acceptability," AIAA Paper 2002-5867, 2002, pp. 1–9.

[11] Clarke, J. P., "A Systems Analysis Methodology for Developing Single Event Noise Abatement Procedures," Ph.D. Dissertation, Massachusetts Institute of Technology, 1997.

[12] Elmer, K., Wat, J., Gershzohn, G., Shivashankara, B., Clarke, J. P., Tan Ho, N., Tobias, L., and Lambert, D., "A Study of Noise Abatement Procedures Using Ames B747-400 Flight Simulator," AIAA Paper 2002-2540, 2002, pp. 1–10.

[13] Erkelens, L. J. J., "Research into New Noise Abatement Procedures for the 21st Century," AIAA Paper 2000-4474, 2000, pp. 1–10.

[14] Koeslag, M. F., "Advanced Continuous Descent Approaches," Faculty of Aerospace Engineering, Delft University of Technology and National Aerospace Laboratory NLR, Technical Rept. NLR-TR-2001-359, 2001.

[15] Ren, L., Clarke, J. P., and Tan Ho, N., "Achieving Low Approach Noise Without Sacrificing Capacity," *Proceedings of the 22nd Digital Avionics Systems Conference (DASC)*, No. 1.E.3 Vol. 1, IEEE, Piscataway NJ, 2003, pp. 1–9.

[16] Elmer, K., Wat, J., Shivashankara, B., Clarke, J. P., Tong, K., Brown, J., and Warren, A., "Community Noise Reduction Using Continuous Descent Approach: A Demonstration Flight Test at Louisville," AIAA Paper 2003-3277, 2003, pp. 1–9.

[17] Tan Ho, N., and Clarke, J. P., "Mitigating Operational Aircraft Noise Impact by Leveraging on Automation Capability," AIAA Paper 2001-5239, 2001, pp. 1–8.

[18] In 't Veld, A. C., van Paassen, M. M., Mulder, M., and Clarke, J. P., "Pilot Support for Separation Assurance During Decelerating Approaches," AIAA Paper 2004-5102, 2005, pp. 1–13.

[19] De Prins, J. L., Schippers, K. F. M., Mulder, M., van Paassen, M. M., in 't Veld, A. C., and Clarke, J. P., "Enhanced Self-Spacing Algorithm for Three-Degree Decelerating Approaches," AIAA Paper 2005-6140, 2005, pp. 1–22.

[20] De Gaay Fortman, W. F., Mulder, M., van Paassen, M. M., in 't Veld, A. C., and Clarke, J. P., "Wind Profile Prediction to Support Three-Degree Decelerating Approaches," AIAA Paper 2005-6141, 2005, pp. 1–23.

[21] Schippers, K. F. M., De Prins, J. L., Mulder, M., van Paassen, M. M., in 't Veld, A. C., and Clarke, J. P., "Investigation of a Three-Degree Decelerating Approach of a Twin Engined Jet Aircraft," AIAA Paper 2005-6139, 2005, pp. 1–28.

[22] Simon, H. A., *Models of Man*, Wiley, New York, 1957.

[23] Boiffier, J. L., *The Dynamics of Flight: The Equations*, Wiley, Chichester, U.K., 1998.

[24] van der Linden, C. A. A. M., "DASMAT—Delft University Aircraft Simulation Model and Analysis Tool," Delft, Technical Rept. LR-781, University of Technology, Delft, The Netherlands, 1996.

[25] Wieringa, J., and Rijkoort, P. J., *Windklimaat van Nederland (in Dutch)*, Staatsuitgeverij, The Hague, The Netherlands, 1983.

[26] Baarspul, M., *Flight Simulation Techniques*, Faculty of Aerospace Engineering, Delft University of Technology, Delft, The Netherlands, 1982.

[27] Hart, S. G., and Staveland, L. E., "Development of NASA-TLX (Task Load Index): Results of empirical and theoretical research," *Human Mental Workload*, edited by P. A. Hancock and N. Meshkati, Elsevier Science Publishers, North–Holland, Amsterdam, 1988, pp. 139–183.